Optimizing the output-photon entanglement in multimode optomechanical systems

Zhi Jiao Deng,[1,2,3,*] Xiao-Bo Yan,[2] Ying-Dan Wang,[2] and Chun-Wang Wu[1,3]

[1]*Department of Physics, College of Science, National University of Defense Technology, Changsha 410073, People's Republic of China*
[2]*State Key Laboratory of Theoretical Physics, Institute of Theoretical Physics, Chinese Academy of Sciences,*
Beijing 100190, People's Republic of China
[3]*Interdisciplinary Center for Quantum Information, National University of Defense Technology,*
Changsha 410073, People's Republic of China

Entangled light beams are important resources for quantum information processing. For some applications like teleportation, only the entanglement between two wave packets (two harmonic oscillators) is needed. So the calculation of output-photon entanglement involves projecting continuous output modes onto wave-packet modes by filter functions, thus resulting in a strong dependence of entanglement on the filter functions. In this paper, we aim at optimizing the filter functions to obtain a large entanglement in a relatively short time, which is important for utilizing the entangled light beams more efficiently in real experiments. We outline the general optimization procedures based on our previous schemes of generating entangled beams in a multimode optomechanical system. Moreover, we give analytic insights into as well as physical explanations of the wave-packet optimization, which are helpful for experimental estimations.

I. INTRODUCTION

Entanglement is a unique feature of quantum mechanics and an important resource for quantum information processing. In order to generate entanglement, the subsystems should have direct or indirect mutual interactions. Optomechanics [1], which deals with the nonlinear interaction between mechanical motion and light modes, can be used to generate various entangled states, including the entanglement between mechanics and light modes [2–6] and between different mechanical motions [7–10] or light modes [11–22]. Recently, the entanglement between a microwave pulse and a mechanical mode was demonstrated in a microwave circuit [23].

Among all the above-mentioned entanglement generations, the two entangled light beams are of particular interest, as the flying photons are ready for subsequent use. There are several schemes [17–22] regarding how to generate entangled light beams in optomechanical systems. The basic ideas are quite similar: two cavity modes get entangled by interacting with the same mechanical mode. Thus the output cavity beams are also entangled with each other. In our previous work [22], we increase the generation efficiency by adding an extra cavity mode. However, the main goal of this article is to define an entanglement rate to characterize the entanglement properties of the two output beams, which is quite different from the usual treatment involving filter functions [24,25]. Usually, filter functions are applied to each cavity output mode [11,14], and then the entanglement between the two filtered modes is calculated by using the logarithmic negativity [26,27]. So the entanglement value depends strongly on the output-photon spectra and the chosen filter functions. The usage of filter functions is due to the fact that in applications like teleportation [14], only the entanglement of two wave packets (two harmonic oscillators) is needed, while the output light beams are continuous modes. For experimentalists, the most desirable outcome is to obtain a large entanglement in a relatively short time interval. So, given a set of physical parameters of the systems, it is natural to ask whether there is a general method to optimize the filter functions to achieve this goal, which is important for guiding experimentalists to better use of the entangled beams.

In this article, we show how to optimize output-photon entanglement. Optimization of the output entanglement has also been discussed in detail in Ref. [22]. But there is an essential difference. In our previous work, we discuss the total entanglement between the two output beams within some long time interval. Then we put forward the new concept of entanglement rate, which is defined as the total entanglement divided by the considered time interval. This measure gives the total entanglement emitted from the source per unit time, which is an inherent property of the source. However, sometimes only some of the signals from the source are needed, for example, we only need the entanglement of two harmonic oscillators in teleportation. This is why we usually project continuous output modes onto wave-packet modes and discuss the entanglement of two filtered wave packets. So the entanglement in this case strongly depends on the filter functions. In a word, our former work discusses the entanglement optimization of two sets of harmonic oscillators, while here we investigate that of two harmonic oscillators. Which optimization is relevant to the experiments depends on the concrete applications. Optimization of the entanglement rate depends only on the physical parameters of the system. Here, the entanglement of two filtered modes relies on the specific form of the filter functions as well as the physical parameters. Our aim is, given a set of physical parameters, to optimize the filter functions to be in the appropriate time intervals and frequency ranges. For simplicity, we can imagine two filtered wave packets coming from the two output modes, respectively. In this case, the physical parameters and the form of the filtered functions are fixed, while the delay time and bandwidth of the filter functions are free to change. To illustrate the main idea of how to optimize

*dengzhijiao926@hotmail.com

these two degrees of freedom, we base our discussions on the scheme in Ref. [22]. However, the optimization method is also applicable to other optomechanical schemes [17–21] and nonlinear systems [28,29]. Our studies show that there is an optimal delay time between the two filtered wave packets. After finding the optimal delay time, the optimal bandwidth (at which the entanglement equals half its maximum) is equal to twice the frequency mismatch δ (see Sec. II) for some intermediate region of δ. Moreover, when we increase the value of δ to be sufficiently large, the optimal bandwidth saturates to a constant limit. The paper is organized as follows: in Sec. II, we briefly review our previous scheme for the generation of entangled light beams and then discuss how to calculate the output entanglement of two filtered wave packets. In Sec. III, we show how to optimize both the wave-packet delay time and the bandwidth to get a larger entanglement in a relatively short time. In Sec. IV, we summarize our results.

II. PHYSICAL SYSTEM

As shown in Fig. 1, we consider a four-mode optomechanical system including three optical cavity modes with equal splitting J and one mechanical mode with frequency Ω. The optomechanical couplings arise from the radiation pressure force, and optical mode a_0 is resonantly driven by a laser. The general Hamiltonian of the whole system is ($\hbar = 1$) [22]

$$\hat{H} = \sum_{q=\pm,0} \omega_q \hat{a}_q^\dagger \hat{a}_q + \Omega \hat{b}^\dagger \hat{b} - \sum_{q,q'=\pm,0} g_{q,q'}^{(0)} \hat{a}_q^\dagger \hat{a}_{q'} (\hat{b} + \hat{b}^\dagger) + \Lambda(\hat{a}_0 e^{i\omega_0 t + \phi} + \text{H.c.}), \quad (1)$$

where $\omega_\pm = \omega_0 \pm J$, $g_{q,q'}^{(0)}$ denotes the optomechanical coupling coefficient, and Λ and ϕ account for the driving amplitude and phase, respectively. This kind of Hamiltonian can be realized in the membrane-in-the-middle setup [30,31] or three coupled optomechanical cells as described in Ref. [22]. We assume that the frequency mismatch $\delta = \Omega - J$ is much smaller than the mechanical frequency Ω, i.e., $|\delta| \ll \Omega$, and
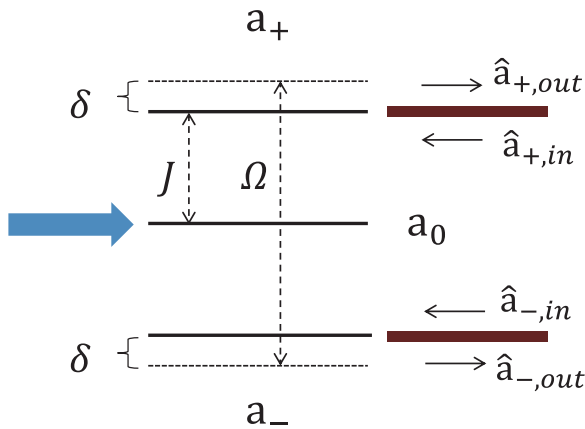
FIG. 1. Schematic level diagram for generating entangled light beams. Three cavity modes with equal frequency distances J are nearest-neighbor coupled by the same mechanical mode of vibrational frequency Ω. The resonant driving of the middle a_0 mode will lead to EPR entanglement between $a_\pm$ modes via photon scatterings. Outgoing modes of $a_\pm$, i.e., $\hat{a}_{\pm,\text{out}}(t)$, constitute entangled light beams.

the mechanical sidebands are resolved, i.e., $\kappa \ll \Omega$, where κ is the intensity damping rate of the optical cavity modes. Under these conditions and a moderate driving strength, only four optomechanical coupling terms, $g_{0,+}^{(0)} \hat{a}_0^\dagger \hat{a}_+ \hat{b}^\dagger + g_{0,-}^{(0)} \hat{a}_0^\dagger \hat{a}_- \hat{b} +$ H.c., dominate. After transformation to the interaction picture with respect to $\hat{H}_0 = \sum_{q=\pm,0} \omega_q \hat{a}_q^\dagger \hat{a}_q + J\hat{b}^\dagger \hat{b}$, the Hamiltonian under the rotating-wave approximation and the standard linearization reads

$$\hat{H}_{\text{lin}} = \delta \hat{b}^\dagger \hat{b} - \frac{g}{2}[(\hat{a}_+^\dagger + \hat{a}_-)\hat{b} + \text{H.c.}], \quad (2)$$

with $g/2 = g_{+,0}^{(0)} \alpha = g_{0,-}^{(0)} \alpha$, $\alpha = \frac{-i\Lambda e^{-i\phi}}{\kappa/2}$. Without loss of generality, g can be chosen as a real number. The effective optomechanical coupling strength should fulfill $|g| \ll \Omega$ to keep the above rotating-wave approximation valid. The physical process to generate entangled light beams goes as follows: one photon in the driven a_0 mode is scattered into the a_- mode while emitting a phonon, then another a_0 photon will absorb this phonon and be scattered into the a_+ mode. So in total, a pair of a_+ and a_- photons will be generated from of a pair of a_0 photons via an intermediate phonon. Thus the effective two-mode squeezing term $\hat{a}_+^\dagger \hat{a}_-^\dagger + \hat{a}_+ \hat{a}_-$ will lead to EPR entanglement between a_+ and a_- modes. The emitted photons from these two modes constitute the entangled light beams. This scheme is more efficient than previous schemes [19–21] in that the driving and the up- and down- conversions will be fully resonant.

To take into account the mode dissipations, we use the standard input-output theory [32] and the quantum Langevin equations are explicitly given by

$$\dot{\hat{a}}_+ = i\frac{g}{2}\hat{b} - \frac{\kappa}{2}\hat{a}_+ - \sqrt{\kappa}\hat{a}_{+,\text{in}}(t),$$

$$\dot{\hat{a}}_-^\dagger = -i\frac{g}{2}\hat{b} - \frac{\kappa}{2}\hat{a}_-^\dagger - \sqrt{\kappa}\hat{a}_{-,\text{in}}^\dagger(t), \quad (3)$$

$$\dot{\hat{b}} = -i\delta\hat{b} + i\frac{g}{2}(\hat{a}_+ + \hat{a}_-^\dagger) - \frac{\Gamma}{2}\hat{b} - \sqrt{\Gamma}\hat{b}_{\text{in}}(t).$$

Here Γ is the mechanical damping rate, and $\hat{a}_{+,\text{in}}(t)$, $\hat{a}_{-,\text{in}}^\dagger(t)$, $\hat{b}_{\text{in}}(t)$ are the input white noise operators. Their mean values satisfy $\langle \hat{a}_{j,\text{in}}(t) \rangle = \langle \hat{b}_{\text{in}}(t) \rangle = 0$, and their correlations fulfill $\langle \hat{a}_{j,\text{in}}(t)\hat{a}_{j',\text{in}}^\dagger(t') \rangle = \delta_{jj'}\delta(t - t')$, $\langle \hat{a}_{j,\text{in}}^\dagger(t)\hat{a}_{j',\text{in}}(t') \rangle = 0$, $\langle \hat{b}_{\text{in}}(t)\hat{b}_{\text{in}}^\dagger(t') \rangle = (n_{\text{th}} + 1)\delta(t - t')$, $\langle \hat{b}_{\text{in}}^\dagger(t)\hat{b}_{\text{in}}(t') \rangle = n_{\text{th}}\delta(t - t')$ with $j,j' = \pm$, and the mean thermal phonon number $n_{\text{th}} = (\exp(\frac{\hbar\Omega}{k_B T}) - 1)^{-1}$. The output-photon modes are related by $\hat{a}_{j,\text{out}}(t) = \sqrt{\kappa}\hat{a}_j(t) + \hat{a}_{j,\text{in}}(t)$. For the resonant driving case, the system is always stable [22] and the stationary solution of Eq. (3) can be easily obtained by the Fourier transformations, i.e., $\hat{a}_+(\omega) = \int_{-\infty}^{\infty} \hat{a}_+(t)e^{i\omega t}dt$, $\hat{a}_+^\dagger(-\omega) = \int_{-\infty}^{\infty} \hat{a}_+^\dagger(t)e^{i\omega t}dt$.

For some applications like teleportation, only output signals within certain time intervals and frequency bandwidths are used [14]. So we need to measure the entanglement of some filtered output modes. To do this, we first project the continuous output modes $\hat{a}_{\pm,\text{out}}(t)$ onto wave-packet modes by using the relations $\hat{a}_{\pm,f} = \int_{-\infty}^{\infty} f_\pm^*(t)\hat{a}_{\pm,\text{out}}(t)dt$, where $f_\pm(t)$ are the filter functions for the $\hat{a}_{+,\text{out}}(t)$ and $\hat{a}_{-,\text{out}}(t)$ modes, respectively. $f_\pm(t)$ fulfill the normalization conditions $\int_{-\infty}^{\infty} |f_\pm(t)|^2 dt = 1$. These filter functions, which contain the information on the time interval and frequency bandwidth,

are realized in experiments by adjusting the temporal mode functions of the local oscillators in homodyne detection [33]. Then we use the logarithmic negativity [26] to calculate the entanglement between two wave packets $\hat{a}_{\pm,f}$. For convenience, we define vector $u = [\hat{x}_{+,f} \ \hat{p}_{+,f} \ \hat{x}_{-,f} \ \hat{p}_{-,f}]^T$ with $\hat{x}_{j,f} = \frac{1}{\sqrt{2}}(\hat{a}_{j,f} + \hat{a}_{j,f}^\dagger)$, $\hat{p}_{j,f} = \frac{1}{\sqrt{2}i}(\hat{a}_{j,f} - \hat{a}_{j,f}^\dagger)$. The entanglement between modes $\hat{a}_{\pm,f}$ is determined by the covariance matrix V with matrix elements $V_{kk'} = \frac{1}{2}\langle u_k u_{k'} + u_{k'} u_k \rangle$. Inserting the stationary solutions of Eq. (3), we have

$$V = \begin{pmatrix} N_+ + \frac{1}{2} & 0 & \mathrm{Re}(X) & \mathrm{Im}(X) \\ 0 & N_+ + \frac{1}{2} & \mathrm{Im}(X) & -\mathrm{Re}(X) \\ \mathrm{Re}(X) & \mathrm{Im}(X) & N_- + \frac{1}{2} & 0 \\ \mathrm{Im}(X) & -\mathrm{Re}(X) & 0 & N_- + \frac{1}{2} \end{pmatrix}, \quad (4)$$

where

$$N_+ = \langle \hat{a}_{+,f}^\dagger \hat{a}_{+,f} \rangle = \int_{-\infty}^{\infty} d\omega |f_+(\omega)|^2 n_+(\omega),$$

$$N_- = \langle \hat{a}_{-,f}^\dagger \hat{a}_{-,f} \rangle = \int_{-\infty}^{\infty} d\omega |f_-(\omega)|^2 n_-(\omega),$$

$$X = \langle \hat{a}_{+,f} \hat{a}_{-,f} \rangle = \int_{-\infty}^{\infty} d\omega f_+^*(\omega) f_-^*(-\omega) x(\omega),$$

with

$$n_+(\omega) = \int_{-\infty}^{\infty} e^{-i\omega t} \langle \hat{a}_{+,\mathrm{out}}^\dagger(t) \hat{a}_{+,\mathrm{out}}(0) \rangle dt$$

$$= \frac{\kappa \Gamma n_{\mathrm{th}}(g/2)^2 (\omega^2 + (\kappa/2)^2) + \kappa^2 (g/2)^4}{((-\omega+\delta)^2 + (\Gamma/2)^2)(\omega^2 + (\kappa/2)^2)^2},$$

$$n_-(\omega) = \int_{-\infty}^{\infty} e^{-i\omega t} \langle \hat{a}_{-,\mathrm{out}}^\dagger(t) \hat{a}_{-,\mathrm{out}}(0) \rangle dt$$

$$= \frac{\kappa \Gamma (n_{\mathrm{th}}+1)(g/2)^2 (\omega^2 + (\kappa/2)^2) + \kappa^2 (g/2)^4}{((\omega+\delta)^2 + (\Gamma/2)^2)(\omega^2 + (\kappa/2)^2)^2},$$

$$x(\omega) = \int_{-\infty}^{\infty} e^{i\omega t} \langle \hat{a}_{+,\mathrm{out}}(t) \hat{a}_{-,\mathrm{out}}(0) \rangle dt$$

$$= \frac{i(-\omega+\delta)\kappa(g/2)^2}{((-\omega+\delta)^2 + (\Gamma/2)^2)(\omega^2 + (\kappa/2)^2)}$$

$$- (n_+(\omega) + n_-(-\omega))/2,$$

and filter functions in the frequency domain $f_j(\omega) = \frac{1}{\sqrt{2\pi}} \int_{-\infty}^{\infty} f_j(t) e^{i\omega t} dt$. Here $n_+(\omega)$ and $n_-(\omega)$ denote the output-photon spectra for the a_+ and a_- modes, respectively, and $x(\omega)$ represents the correlation between the ω component in the $\hat{a}_{+,\mathrm{out}}(t)$ mode and the $-\omega$ component in the $\hat{a}_{-,\mathrm{out}}(t)$ mode. These two components satisfy the energy conservation laws since their frequency sum equals twice the driven mode frequency. The logarithmic negativity is defined as $E = \max(0, -\log(2\eta_-))$, with η_- being the smaller symplectic eigenvalue of the partial transpose of matrix V. Its analytical expression is too cumbersome to show here. There is an interesting limiting case, i.e., when the bandwidths of both filter functions go to 0 and only single frequencies are considered. In this case, only the components satisfying energy conservation have nonzero correlations and thus nonzero entanglement. The entanglement among different single-frequency components is then fully described by the spectral density of entanglement

$E_s(\omega)$, which gives the logarithmic negativity between the ω component in the $\hat{a}_{+,\mathrm{out}}(t)$ mode and the $-\omega$ component in the $\hat{a}_{-,\mathrm{out}}(t)$ mode. Instead, for a finite bandwidth, the matrix elements in V are some mean values over certain frequency regions, and the filter functions determine the weight functions in this averaging. With the right choice of filter functions, we can generate a large output entanglement in a relatively short time.

III. OPTIMIZATION Of THE OUTPUT-PHOTON ENTANGLEMENT

Before optimizing the output-photon entanglement, we check some properties of the output-photon spectrum $n_\pm(\omega)$. The ω component in the interaction picture actually accounts for the $\omega_\pm + \omega$ physical components for the $\hat{a}_{+,\mathrm{out}}(t)$ and $\hat{a}_{-,\mathrm{out}}(t)$ modes, respectively. As shown in Fig. 2(a), there are typically two peaks separated roughly by frequency δ in the spectrum. For the $\hat{a}_{\pm,\mathrm{out}}(t)$ modes, one peak is centered around $\omega \simeq 0$, with width κ, and the other is around $\omega \simeq \pm\delta$, with width Γ. The peak around $\omega \simeq 0$ is dominated by contributions from optical vacuum noise, while the peak around $\omega \simeq \pm\delta$ is mainly generated by mechanical thermal noise. Thus the former is more robust to mechanical thermal fluctuations and has larger entanglement. This is illustrated in Fig. 2(b), where we plot the spectral density of entanglement $E_s(\omega)$. It also has two peaks in the same positions as in the output-photon spectrum, and the one around $\omega \simeq 0$ is higher due to its immunity to the mechanical thermal noise. So we would choose our filter functions $f_\pm(\omega)$ to be centered around $\omega = 0$.
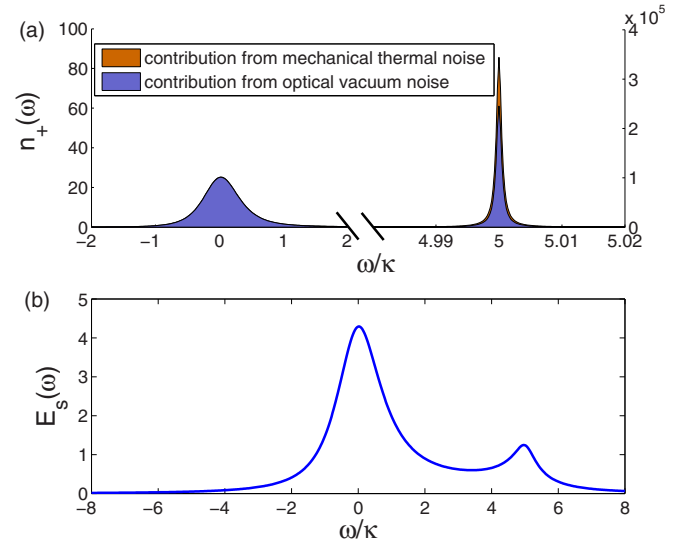
FIG. 2. (a) Output photon spectrum $n_+(\omega)$ for the upper optical mode with $g/\kappa = 1$, $\Gamma/\kappa = 0.001$, $\delta/\kappa = 5$, $n_{\mathrm{th}} = 100$. Contributions from the optical vacuum noise and mechanical thermal noise are distinguished by different colors. (b) Spectral density of entanglement $E_s(\omega)$, i.e., the logarithmic negativity between the ω component in the $\hat{a}_{+,\mathrm{out}}(t)$ mode and the $-\omega$ component in the $\hat{a}_{-,\mathrm{out}}(t)$ mode. These two components can be obtained by the filter functions centered around $\pm\omega$, respectively, and both with a bandwidth approaching 0.
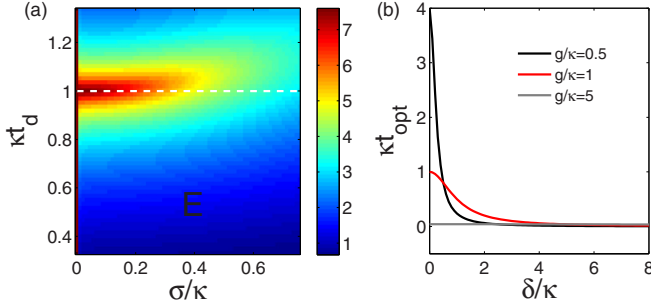
FIG. 3. (a) Entanglement as a function of the dimensionless bandwidth σ/κ and time delay κt_d for $g/\kappa = 1$, $\Gamma/\kappa = 0.001$, $\delta/\kappa = 0$, $n_{\text{th}} = 0$. The dashed white line is the optimal delay time produced by Exp. (6). (b) Optimal delay time κt_{opt} with respect to the frequency mismatch δ/κ under different driving strengths g/κ with $\Gamma/\kappa = 0.001$, $n_{\text{th}} = 0$.

Let us assume that the two filter functions for both output modes have the same bandwidth σ but a delay time t_d, i.e., $f_+(\omega) = e^{i\omega t_d}/\sqrt{\sigma}$, $f_-(\omega) = 1/\sqrt{\sigma}$ for $\omega \in [-\frac{\sigma}{2}, \frac{\sigma}{2}]$, and otherwise, $f_{\pm}(\omega) = 0$. Their Fourier transformations read $f_+(t) = \sqrt{\frac{\sigma}{2\pi}} \frac{\sin(\sigma(t-t_d)/2)}{\sigma t/2}$, $f_-(t) = \sqrt{\frac{\sigma}{2\pi}} \frac{\sin(\sigma t/2)}{\sigma t/2}$, which means that wave packet $\hat{a}_{+,f}$ arrives a time t_d later than wave packet $\hat{a}_{-,f}$. In Fig. 3(a), we plot the two-wave-packet entanglement as a function of the dimensionless bandwidth σ/κ and time delay κt_d. We can see that with increasing bandwidth, the entanglement decreases almost monotonically. When $\sigma/\kappa \ll 1$, the entanglement has its maximum value and is independent of t_d, since a small bandwidth means a long duration of the wave packet, thus a finite time delay κt_d will not affect the results. However, there exists an optimal delay time t_{opt} at which the entanglement can decrease relatively slowly when the bandwidth increases. To determine the t_{opt}, we can check the matrix element $X = \langle \hat{a}_{+,f} \hat{a}_{-,f} \rangle$, which accounts for the correlation between the two wave packets. We expect that a larger correlation X would lead to larger entanglement. After inserting the filter functions, we have

$$X = \frac{1}{\sigma} \int_{-\sigma/2}^{\sigma/2} d\omega\, e^{-i\omega t_d} x(\omega)$$

$$= \frac{1}{\sigma} \int_{-\sigma/2}^{\sigma/2} d\omega\, e^{-i\omega t_d} |x(\omega)| e^{i(\varphi(0) + \frac{d\varphi(\omega)}{d\omega}|_{\omega=0}\omega + \dots)}. \quad (5)$$

Here we have expanded the phase function $\varphi(\omega)$ of $x(\omega)$ in a Taylor series around $\omega = 0$. When σ increases from 0 but is within the region in which $\varphi(\omega)$ is linear with respect to ω, to adjust $t_d = \frac{d\varphi(\omega)}{d\omega}|_{\omega=0}$ would eliminate the integrand's phase dependence on ω, leading to an enhanced value of X. So the optimal delay time t_{opt} is found to be $\frac{d\varphi(\omega)}{d\omega}|_{\omega=0}$, and more explicitly,

$$t_{\text{opt}} = \frac{C + n_{\text{th}} + \frac{1}{2}}{\Gamma\left(\left(C + n_{\text{th}} + \frac{1}{2}\right)^2 + \left(\frac{\delta}{\Gamma}\right)^2\right)}, \quad (6)$$

with the cooperativity $C = \frac{g^2}{\kappa\Gamma}$. The dashed white line in Fig. 3(a) is predicted by this formula. When the driving is sufficiently large, i.e., $C \gg n_{\text{th}} + 1/2$, the dimensionless

optimal delay time is approximately given by

$$\kappa t_{\text{opt}} \simeq \frac{(g/\kappa)^2}{(g/\kappa)^4 + (\delta/\kappa)^2}. \quad (7)$$

There are two special cases: one is on-resonance, i.e., $\delta = 0$, and $t_{\text{opt}} \simeq \frac{1}{\kappa(g/\kappa)^2}$. In this case, the entangled photon pairs will be emitted earlier in the $\hat{a}_{-,\text{out}}(t)$ mode than in the $\hat{a}_{+,\text{out}}(t)$ mode, which accounts for the down-conversion happening before the up-conversion. In fact, the processes also occur in the reversed order, but this does not contribute to entanglement. As we explained above, the down-conversion produces a phonon, which is subsequently absorbed in the up-conversion. So the generated photon pairs are connected by the same intermediate phonon. However, in the reversed order, these two scatterings happen independently and the scattered photons are not correlated. Thus the optimal delay time reflects the microscopic picture of generating entangled photon pairs. The stronger the driving, the less the time needed for photon scattering, and the time interval between the two wave packets becomes shorter. Another interesting case is the large-detuning case, i.e., $\delta \gg g$ and $t_{\text{opt}} \simeq 0$, which corresponds to photon scatterings via a virtual intermediate phonon, and the up- and down-conversions happen at the same time. In Fig. 3(b), we plot the optimal delay time κt_{opt} versus the frequency mismatch δ/κ with different driving strengths g/κ. The maximum value $1/(g/\kappa)^2$ is achieved on-resonance, and the curves decrease to half the maximum at $\delta/\kappa = (g/\kappa)^2$ and approach 0 when $\delta \gg g$. These curves will not be influenced by increasing n_{th}, if n_{th} is much smaller than the cooperativity C.

Although large entanglement can be achieved with a small bandwidth, the generation efficiency is low due to the long wave-packet duration, $\tau = 2\pi/\sigma$, which is inversely proportional to σ. Besides optimizing the wave-packet delay time, it is also necessary to optimize its bandwidth and make it as large as possible. At a fixed optimal delay time, we first check how the entanglement changes with the bandwidth. In Fig. 4(a), we plot the ratio of entanglement E to its maximum $E_{\text{max}}(\delta)$ with respect to σ/κ for different choices of δ/κ. The maximum $E_{\text{max}}(\delta)$ is reached in the limit of $\sigma = 0$ and decreases with increasing δ/κ due to the reduced peak height in the output-photon spectrum. The curves of $E/E_{\text{max}}(\delta)$ versus σ/κ decrease almost monotonically but show a sudden jump at $\sigma/\kappa \simeq 2\delta/\kappa$. This behavior can be understood by noting that, as we increase the bandwidth, at some point it will include the narrow and high peaks around $\omega = \pm\delta$ [see Fig. 2(a)], and they will suddenly dominate the entanglement properties. The main problem here is how to define the optimal bandwidth. If we want to get a large entanglement in a short time, we might be interested in the bandwidth at which we can optimize the ratio E/τ. However, the problem is that in many cases, we get a maximum value of E/τ when τ is very small. The ratio is high, however, the entanglement is small given a small τ. Another possibility is to define the optimal bandwidth σ_{opt} as half height width of the above curves, i.e., $E(\sigma_{\text{opt}}/\kappa)/E_{\text{max}}(\delta) = 0.5$. By this definition, the entanglement only decreases by half the maximum, so we can guarantee the amount of entanglement. Here, we adopt this second definition and analyze its behavior with different parameters. If the jump happens to intersect with the dashed
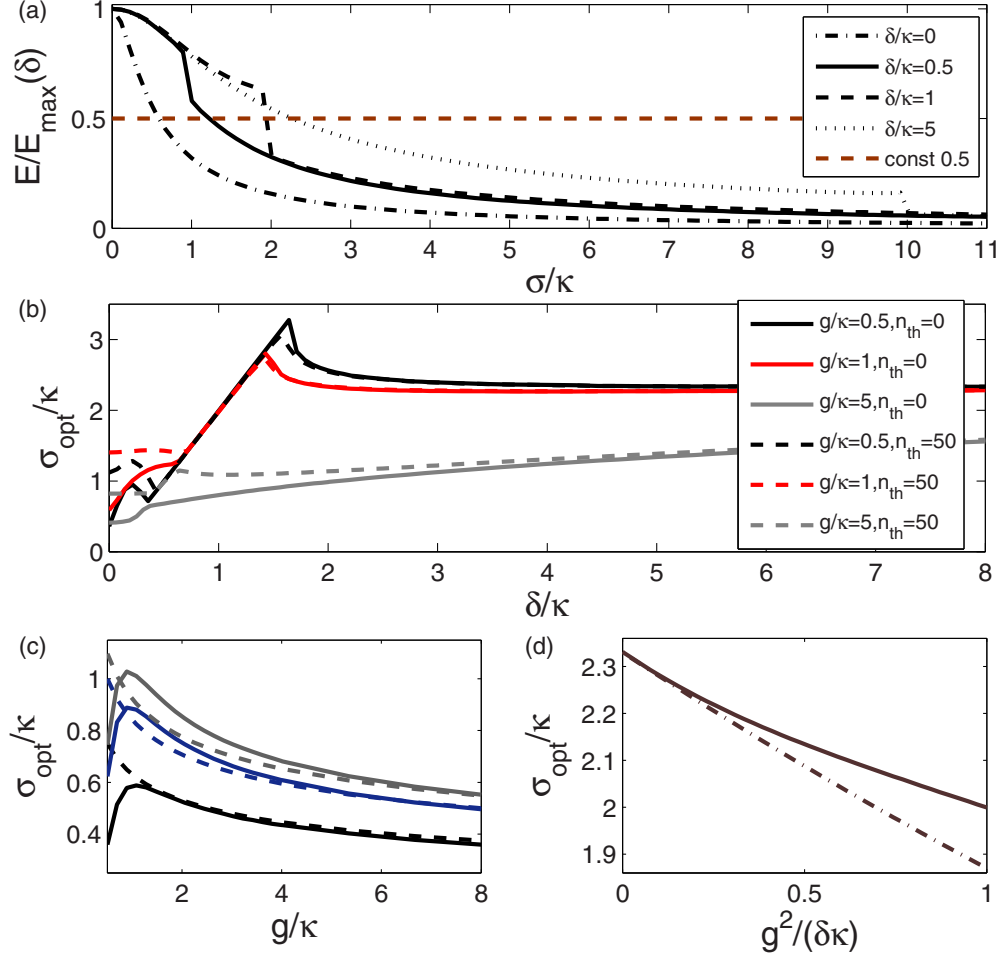
FIG. 4. (a) Ratio of entanglement to maximum entanglement, i.e., $E/E_{\max}(\delta)$, as a function of the dimensionless bandwidth σ/κ with different frequency mismatches δ/κ for $g/\kappa = 1$, $\Gamma/\kappa = 0.001$, $n_{\mathrm{th}} = 0$. (b) Dimensionless optimal bandwidth $\sigma_{\mathrm{opt}}/\kappa$ versus frequency mismatch δ/κ with different driving strengths and thermal phonon numbers at fixed $\Gamma/\kappa = 0.001$. (c) Optimal bandwidth $\sigma_{\mathrm{opt}}/\kappa$ as a function of the driving strength g/κ for the resonant case, i.e., $\delta/\kappa = 0$, with different combinations of Γ/κ and n_{th} (black, $\Gamma/\kappa = 0.001$, $n_{\mathrm{th}} = 0$; blue, $\Gamma/\kappa = 0.01$, $n_{\mathrm{th}} = 0$; gray, $\Gamma/\kappa = 0.001$, $n_{\mathrm{th}} = 10$); solid lines represent numerical results, while dashed lines were given by $\sigma_{\mathrm{opt}}/\kappa = (25(1 + 2n_{\mathrm{th}})/C)^{1/8}$. (d) Optimal bandwidth $\sigma_{\mathrm{opt}}/\kappa$ versus dimensionless parameter $g^2/(\delta\kappa)$ in the adiabatic model, shown by the solid line. Analytic approximation $(23/8)^{4/5} e^{-\frac{11}{50} g^2/(\delta\kappa)}$ in the vicinity of $g^2/(\delta\kappa) = 0$, indicated by the dash-dotted line.

0.5 constant line, then $\sigma_{\mathrm{opt}}/\kappa \simeq 2\delta/\kappa$, while the cases where the jump occurs above and below lead to $\sigma_{\mathrm{opt}}/\kappa > 2\delta/\kappa$ and $\sigma_{\mathrm{opt}}/\kappa < 2\delta/\kappa$, respectively. This feature is reflected by the solid red line in Fig. 4(b), where the linear region originates from the intersecting case. The existence of this linear region is quite general for different parameters if $\Gamma/\kappa \ll 1$, which is also common in real experiments [1,30,31,34–36].

As above, we also give analytic predictions for two special cases: for the resonant case, i.e., $\delta = 0$, and under the strong driving conditions $C \gg n_{\mathrm{th}} + 1/2$, we have $\sigma_{\mathrm{opt}}/\kappa \simeq (25(1 + 2n_{\mathrm{th}})/C)^{1/8}$. We compare this formula with the numerical results in Fig. 4(c) and see that when $C/(n_{\mathrm{th}} + 1/2) > 10^3$, these two results agree very well. In the large-detuning case, i.e., when $\delta \gg \kappa, \Gamma, g$, we could adiabatically eliminate the mechanical modes to get the simplified Hamiltonian $\hat{H}_{\mathrm{ad}} = \delta \hat{b}^\dagger \hat{b} - \frac{g^2}{4\delta}(\hat{a}_+^\dagger \hat{a}_+ + \hat{a}_-^\dagger \hat{a}_- + \hat{a}_+^\dagger \hat{a}_-^\dagger + \hat{a}_+ \hat{a}_-)$. Thus all the entanglement properties are determined solely by $g^2/(\delta\kappa)$. In Fig. 4(d), we plot the optimal bandwidth $\sigma_{\mathrm{opt}}/\kappa$ as a function of $g^2/(\delta\kappa)$ in the adiabatic model. This is done by starting from

the effective Hamiltonian $\hat{H}_{\mathrm{ad}}$ and performing a numerical search. If δ is large enough to make $g^2/(\delta\kappa) \ll 1$, the behavior of the optimal bandwidth is indicated by the dash-dotted-line relation $(23/8)^{4/5} e^{-\frac{11}{50} g^2/(\delta\kappa)}$ up to $g^2/(\delta\kappa) \simeq 0.1$. This relation predicts that all the curves in Fig. 4(b) will ultimately reach the limiting value $(23/8)^{4/5} \simeq 2.33$.

IV. CONCLUSION

In summary, we have shown how to optimize output-photon entanglement based on our previous scheme. Our goal is, given a set of physical parameters, to determine how to optimally filter out two wave packets (two harmonic oscillators) from the entangled light beams. The method presented here applies to other optomechanical schemes [17–21] and nonlinear systems such as the Kerr medium [28] and Josephson parametric converter [29]. We first consider the output-photon spectrum to determine the frequency region where there are high photon number densities and a small effect of the mechanical thermal

noise (this noise is only for optomechanical systems). We then choose a filter function centered around the spectral peak in this region and introduce a delay time between the two wave packets. The wave-packet entanglement will generally decrease monotonically with increasing bandwidth due to the averaging effects in the covariance matrix. However, there exists an optimal delay time, at which the entanglement decreases relatively slowly. At this optimal delay time, we discuss the optimal bandwidth, at which the entanglement decreases to half its maximum. There are several interesting features of the optimization: (i) The optimal delay time reflects the second-order process for generating entangled photon pairs. For the resonant case, the up-conversion comes after the down-conversion, while for the large-detuning case, they happen at the same time. The time differences for these two processes are captured by the optimal delay time. (ii) At the optimal delay time, the entanglement decreases with increasing bandwidth; in particular, a sudden jump appears at $\sigma \simeq 2\delta$, which is a common phenomenon for $\Gamma \ll \kappa$ and gives rise to a linear relation $\sigma_{\text{opt}} \simeq 2\delta$ for some intermediate region of δ/κ. (iii) When the frequency mismatch δ is

much larger than all the other characteristic parameters, the entanglement is fully determined by $g^2/(\delta\kappa)$. The optimal bandwidth $\sigma_{\text{opt}}/\kappa$ goes to a limiting value, 2.33, when $g^2/(\delta\kappa)$ approaches 0. In addition, we give some analytic results for wave-packet optimization with the aim of facilitating experimental estimations. To obtain a large entanglement in a relatively short time is experimentally feasible and important, and we believe that our study is quite useful for applications relying on entangled light beams.

[1] M. Aspelmeyer, T. J. Kippenberg, and F. Marquardt, Rev. Mod. Phys. **86**, 1391 (2014).

[2] D. Vitali, S. Gigan, A. Ferreira, H. R. Böhm, P. Tombesi, A. Guerreiro, V. Vedral, A. Zeilinger, and M. Aspelmeyer, Phys. Rev. Lett. **98**, 030405 (2007).

[3] A. Mari and J. Eisert, Phys. Rev. Lett. **103**, 213603 (2009).

[4] S. G. Hofer, W. Wieczorek, M. Aspelmeyer, and K. Hammerer, Phys. Rev. A **84**, 052327 (2011).

[5] U. Akram, W. Munro, K. Nemoto, and G. J. Milburn, Phys. Rev. A **86**, 042306 (2012).

[6] M. Eghbali-Arani, H. Yavari, M. A. Shahzamanian, V. Giovannetti, and Sh. Barzanjeh, J. Opt. Soc. Am. B **32**, 798 (2015).

[7] S. Bose, K. Jacobs, and P. L. Knight, Phys. Rev. A **56**, 4175 (1997).

[8] J. Zhang, K. Peng, and S. L. Braunstein, Phys. Rev. A **68**, 013808 (2003).

[9] M. J. Hartmann and M. B. Plenio, Phys. Rev. Lett. **101**, 200503 (2008).

[10] M. Schmidt, M. Ludwig, and F. Marquardt, New J. Phys. **14**, 125005 (2012).

[11] C. Genes, A. Mari, P. Tombesi, and D. Vitali, Phys. Rev. A **78**, 032316 (2008).

[12] C. Wipf, T. Corbitt, Y. Chen, and N. Mavalvala, New J. Phys. **10**, 095017 (2008).

[13] Sh. Barzanjeh, D. Vitali, P. Tombesi, and G. J. Milburn, Phys. Rev. A **84**, 042342 (2011).

[14] Sh. Barzanjeh, M. Abdi, G. J. Milburn, P. Tombesi, and D. Vitali, Phys. Rev. Lett. **109**, 130503 (2012).

[15] Sh. Barzanjeh, S. Pirandola, and C. Weedbrook, Phys. Rev. A **88**, 042331 (2013).

[16] Y.-D. Wang and A. A. Clerk, Phys. Rev. Lett. **110**, 253601 (2013).

[17] Z.-q. Yin and Y.-J. Han, Phys. Rev. A **79**, 024301 (2009).

[18] H.-t. Tan and G.-x. Li, Phys. Rev. A **84**, 024301 (2011).

[19] L. Tian, Phys. Rev. Lett. **110**, 233602 (2013).

[20] M. C. Kuzyk, S. J. van Enk, and H. Wang, Phys. Rev. A **88**, 062341 (2013).

[21] Y.-D. Wang, S. Chesi, and A. A. Clerk, Phys. Rev. A **91**, 013807 (2015).

[22] Z. J. Deng, S. J. M. Habraken, and F. Marquardt, arXiv:1406.7815v2.

[23] T. A. Palomaki, J. D. Teufel, R. W. Simmonds, and K. W. Lehnert, Science **342**, 710 (2013).

[24] S. J. van Enk and C. A. Fuchs, Phys. Rev. Lett. **88**, 027902 (2001).

[25] D. Vitali1, P. Cañizares, J. Eschner, and G. Morigi, New J. Phys. **10**, 033025 (2008).

[26] G. Vidal and R. F. Werner, Phys. Rev. A **65**, 032314 (2002).

[27] J. Eisert and M. B. Plenio, Int. J. Quantum Inf. **01**, 479 (2003).

[28] Z. Y. Ou, S. F. Pereira, H. J. Kimble, and K. C. Peng, Phys. Rev. Lett. **68**, 3663 (1992).

[29] F. Schackert, A. Roy, M. Hatridge, M. H. Devoret, and A. D. Stone, Phys. Rev. Lett. **111**, 073903 (2013).

[30] J. D. Thompson, B. M. Zwickl, A. M. Jayich, F. Marquardt, S. M. Girvin, and J. G. E. Harris, Nature **452**, 72 (2008).

[31] J. C. Sankey, C. Yang, B. M. Zwickl, A. M. Jayich, and J. G. E. Harris, Nat. Phys. **6**, 707 (2010).

[32] C. W. Gardiner and M. J. Collett, Phys. Rev. A **31**, 3761 (1985).

[33] D. F. Walls and G. J. Milburn, *Quantum Optics*, 2nd ed. (Springer-Verlag, Berlin, 2008).

[34] J. Chan, T. P. M. Alegre, A. H. Safavi-Naeini, J. T. Hill, A. Krause, S. Gröblacher, M. Aspelmeyer, and O. Painter, Nature (London) **478**, 89 (2011).

[35] E. Verhagen, S. Deléglise, S. Weis, A. Schliesser, and T. J. Kippenberg, Nature **482**, 63 (2012).

[36] D. Kleckner, B. Pepper, E. Jeffrey, P. Sonin, S. M. Thon, and D. Bouwmeester, Opt. Express **19**, 19708 (2011).